

Journal of Materials Chemistry A

Accepted Manuscript



This is an *Accepted Manuscript*, which has been through the Royal Society of Chemistry peer review process and has been accepted for publication.

Accepted Manuscripts are published online shortly after acceptance, before technical editing, formatting and proof reading. Using this free service, authors can make their results available to the community, in citable form, before we publish the edited article. We will replace this *Accepted Manuscript* with the edited and formatted *Advance Article* as soon as it is available.

You can find more information about *Accepted Manuscripts* in the [Information for Authors](#).

Please note that technical editing may introduce minor changes to the text and/or graphics, which may alter content. The journal's standard [Terms & Conditions](#) and the [Ethical guidelines](#) still apply. In no event shall the Royal Society of Chemistry be held responsible for any errors or omissions in this *Accepted Manuscript* or any consequences arising from the use of any information it contains.



Design of nitride semiconductors for solar energy conversion

Andriy Zakutayev^a

Received 00th January 20xx,
Accepted 00th January 20xx

DOI: 10.1039/x0xx00000x

www.rsc.org/

Nitride semiconductors are a promising class of materials for solar energy conversion applications, such as photovoltaic and photoelectrochemical cells. Nitrides can have better solar absorption and electrical transport properties than the more widely studied oxides, as well as potential for better scalability than other pnictides or chalcogenides. In addition, nitrides are also relatively unexplored compared to other chemistries, so they provide a great opportunity for new materials discovery. This paper reviews the recent advances in the design of novel semiconducting nitrides for solar energy conversion technologies. Both binary and multinary nitrides are discussed, with a range of metal chemistries (Cu_3N , ZnSnN_2 , Sn_3N_4 etc) and crystal structures (delafossite, perovskite, spinel etc), including a brief overview of wurtzite III-N materials and devices. The current scientific challenges and promising future directions in the field are also highlighted.

1. Introduction

Conversion of sunlight into electrical energy is one of the most promising routes to meet the 30 TW global electricity demand by 2050. Photovoltaic (PV) solar cell technologies currently provide 0.1 TW of power and are on track to be producing 1 TW by 2025. However, at the >1 TW level of electrical energy production, concerns remain about the sustainability of the growth of the Si solar cell manufacturing,¹ as well as the availability of critical chemical elements for thin-film PV technologies². In addition, storing electricity using batteries for later use, or converting it to fuels for mobile applications, presents an even greater challenge than reaching 30 TW. Hence, new solar cell absorbers are needed, for photoelectrochemical (PEC) fuels production in particular: this is the area where the lack of suitable semiconductor materials is much more pressing than for PV electricity generation. The solar absorber materials used in these novel technologies should be inexpensive, efficient, and reliable like current technologies, but should also be easily scalable to multi-TW levels without constraint.

Semiconducting nitrides are an interesting family of inorganic compounds for optoelectronic applications because of their mixed covalent/ionic bonding properties (Fig. 1) due to moderate electronegativity of the N atom ($\chi_N=3.0$). On one hand, nitrides are more ionic compared to other pnictides ($\chi_{pn}=2.0-2.2$ for pnictogen atoms) studied for solar energy conversion (e.g. GaAs, InGaP₂), so they allow for greater tolerance to structural defects. This is because the constituent atomic orbitals in the ionic compounds lie closer to the band edges than in covalent compounds, so the defect states that result from breaking the atomic bonds would be shallower.

This ionic character of the semiconducting nitrides should result in the potential for good scalability using low-cost materials processing, such as nitride film sputtering integrated into one process line with vacuum deposition of other materials in the device stack. Prior commercial examples of nitride films prepared by in-line sputtering include metallic TiN and other transition metal nitrides used for wear-resistant coatings and architectural glass applications.³

On the other hand, nitrides are more covalent than the oxides ($\chi_O=3.5$) due to the higher position of N 2p compared to O 2p orbitals (Fig. 1). The lower energy difference with electronic states of the metal elements and the resulting better hybridization usually leads to better charge-transport properties and a higher valence band position—and hence lower bandgaps and easier p-type doping⁴ compared to the oxides studied for PV⁵ and PEC⁶ applications. This more covalent character of the nitrides have led to many commercial optoelectronic applications such as light-emitting diodes (LEDs)⁷, photodetectors and laser diodes, as well as numerous electronic devices including high electron mobility transistors (HEMT)⁸ and wide-bandgap power electronics, all based on GaN and related materials.

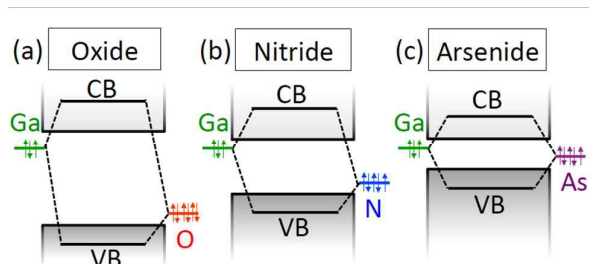


Fig. 1. Schematic representation of chemical bonding in Ga-based semiconducting (a) oxides, (b) nitrides and (c) arsenides, showing how nitrides tend to have intermediate energy of the valence band compared to the more ionic oxides and the more covalent pnictides

^aNational Renewable Energy Laboratory, Golden, Colorado 80401, USA.
E-mail: andriy.zakutayev@nrel.gov

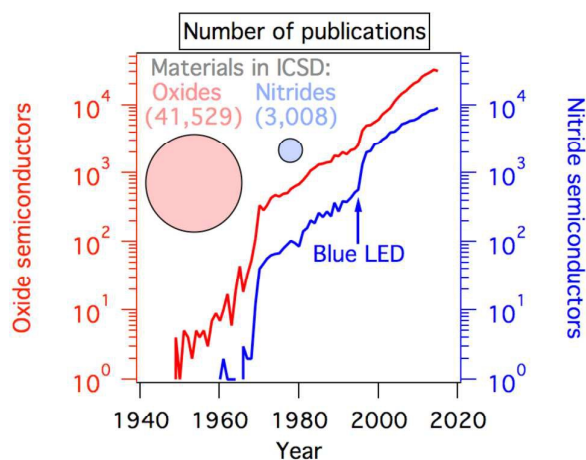


Fig. 2. Number of indexed publications in Scopus in the fields of semiconducting oxides and nitrides as a function of year, demonstrating the increased importance of these materials in electronic applications. Inset: the number of entries in ICSD, proportional to the area of the circles, also illustrates the relatively unexplored character of the nitrides (3,008) compared to the oxides (41,529).

Nitride materials are also interesting from the perspective of basic science because they constitute a relatively unexplored and very diverse class of inorganic compounds (Fig. 2). For example, the inset in Fig. 2 illustrates that in the Inorganic Crystal Structure Database (ICSD), for every nitride (3,008 total entries) there are more than ten oxides (41,529 total entries). Similar trends hold for the number of published papers cataloged in the Scopus Database, as shown in Fig. 2. As a consequence, new nitride materials with structural motifs and crystal structures that have never been reported previously in any other chemistry are discovered with amazing regularity.⁹ Electronic structures and physical properties of even some very simple binary nitrides have yet to be reported (e.g., Sb-N, Bi-N) or have only recently been reported (e.g., Pt-, Ir-nitrides).¹⁰ In part, the uniqueness of the nitride crystal structures can be attributed to the high valence (-3) of a nitrogen element in the compound, and hence, the need for either a high valence of metal elements or a larger number of them per formula unit. This leads to difficulty in satisfying the known stoichiometries/structures with large anion/cation ratios (e.g., A_2BX_4 spinels, ABX_3 perovskites) and to a large number of known “interstitial” nitride compounds.⁹

The relatively unexplored character of the nitride solid-state chemistry may be partially attributed to the *apparently* less stable character of the nitrides compared to oxides, as suggested by more positive nitride formation enthalpies (Fig. 3a). The stability range of a metal nitride M_xN_y is:

$$\Delta H_f(M_xN_y) < x\Delta\mu(M) + y\Delta\mu(N_2)/2 \quad (1)$$

where $\Delta\mu$ are chemical potentials of solid metal M and nitrogen gas N_2 in their standard reference states. It is important to understand that the nitrides are *apparently* less

stable than oxides due to the extremely low energy of the N_2 molecule (low $\Delta\mu(N_2) = -10$ eV, right-hand side of Eq. 1) that is used as a reference state for determining formation enthalpies (compare to the O_2 molecule at $\Delta\mu(O_2) = -6$ eV). It is stressed here that this apparent metastability of the nitrides is *not* due to the weakness of the metal-nitrogen bonds (not high ΔH_f on left-hand side of Eq. 1), which can be as strong or even stronger than the metal-oxygen bonds. Indeed, as shown in Fig. 3b, if the atomic nitrogen chemical potential is used as a reference, the nitrides are as stable as the oxides. Empirically, this notion is supported by the nitride commercial application as hard coatings.³ However, note that this argument (Fig. 3) assumes that there are other kinetic barriers, such as a self-terminating native oxide layer (e.g., Al_2O_3 on AlN) that prevents reaction with the oxygen-containing ambient atmosphere and other possible nitride decomposition pathways.

This review article discusses recent progress in the design of semiconducting nitrides for solar energy conversion, beyond the well-studied case of III-N. The review focuses on the nitrides with potential for photovoltaic and photoelectrochemical applications, and highlights prior examples of research by the author and other researchers in the field. This article also briefly reviews III-N materials as the only class of nitrides with the reported PV device efficiencies. The remainder of the paper is outlined as follows. After a brief general methods section, this review discusses the recent progress in binary nitrides of Cu, Ta, Sn, Ga groups, and related alloys, arranged by metal chemistry. Then, ternary nitride materials are discussed arranged by crystal structure, e.g., delafossites, perovskites, wurtzites, and others that emerge from theoretical predictions. Finally, future research and development directions and the outstanding scientific challenges are highlighted.

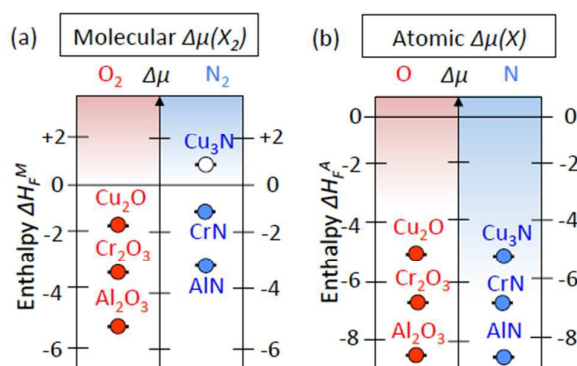


Fig. 3. Schematic representation of the enthalpies of formation for several *s*-, *p*- and *d*-block oxides and nitrides with respect to (a) molecular and (b) atomic nitrogen chemical potentials. This comparison illustrates that the apparent metastability of the nitrides results from the very low energy of the N_2 molecule rather than the weakness of the metal-nitrogen bond.

2. Methods

The promise for good optoelectronic properties (Fig. 1) and the unexplored character (Fig. 2) of the nitrides make them good candidates for “Materials Design” methods. Broadly defined, materials design is aimed at discovering new materials with targeted properties, and is one of the five Grand Challenges for basic energy sciences.¹¹ The related Materials Genome Initiative in the USA¹² and similar governmental programs in other countries, seek to accelerate the rate at which new materials are introduced into the market, beyond the slow and serendipitous approaches of traditional materials science. A key idea behind the materials design is to leverage the modern high-throughput methods from other scientific fields, such as parallelized calculations¹³ from computer sciences, and combinatorial experimentation¹⁴ from pharmaceutical industry. To date, the materials design strategy has been quite fruitful for many researchers, with success stories in our group ranging from experimentally realizing computationally predicted materials¹⁵ in basic science, to identifying¹⁶ and integrating¹⁷ new PV materials (both absorbers and contacts) in applied technology.

Designing novel semiconducting nitrides for solar energy conversion and other applications also presents formidable scientific challenges for both experiments and computations. The main computational challenge is the aforementioned diverse structures and high-integer stoichiometries of the nitrides. These characteristics make it difficult to apply the conventional structure prediction methods based on structure prototyping and genetic algorithms. The problem is exacerbated by the small number of previously reported nitrides, and hence, insufficient training sets for the structure

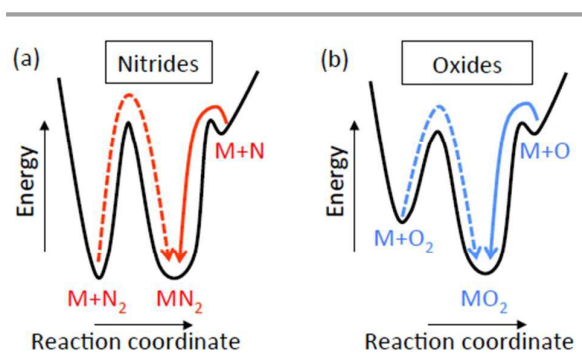


Fig. 4 Generalized potential energy landscape for synthesis of (a) nitrides and (b) oxides, showing a larger kinetic barrier for the synthesis of nitrides from N_2 molecule, but the same barrier if N atom is used. Hence the nitrides may be more difficult to synthesize than the oxides (triple N_2 vs. double O_2 bonds, different left potential wells/barriers), but once made they are as stable as oxide (strong M-N bonds, similar middle potential wells/barriers). Both oxides and nitrides are equally easy to synthesize from high-energy atomic precursors (similar right potential wells/barriers)

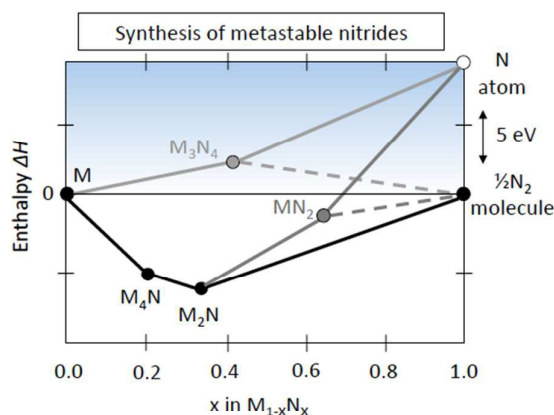


Fig. 5. The “convex hull” diagram for the nitrides that are thermodynamically stable (e.g., M_4N , M_2N , solid black lines) and unstable (e.g., M_3N_4 , MN_2 , dashed gray lines) with respect to the molecular nitrogen N_2 . In comparison, MN_2 and M_3N_4 are metastable with respect to the atomic nitrogen N (solid gray lines) and can be synthesized from high-energy nitrogen precursors, such as N-atom plasma during thin-film sputtering, as shown in Fig. 4

prediction approaches based on data mining; so all these theoretical methods have to be modified to provide reliable predictions.

The main experimental challenge is the synthesis process, given the nitride stability considerations presented above from the thermodynamic point of view (Fig. 3a). For nitride synthesis, the nitrogen triple bond needs to be broken before the reaction with the metal precursors occurs (Fig. 4a, left well), which costs more energy than for the double-bond of the corresponding oxide (Fig. 4b, left well). However, once the metal-nitrogen bond is established, the nitride becomes as stable as the corresponding oxide (Fig. 3b and Fig. 4 middle wells). So in this sense the schematic picture presented in Fig. 3b is just a way to understand the kinetic stability of the synthesized nitrides using simple thermodynamic concepts (such as heats of formation and chemical potentials), without explicitly considering the difficult-to-compute oxidation- or decomposition energy barriers (Fig. 4).

As shown in Fig. 5, metastable nitrides can be synthesized using nitrogen precursors that are higher in energy than the N_2 molecule (Fig. 4 right wells). The physical means often used to achieve high reactivity of nitrogen during the synthesis are (1) unintentional cracking of N_2 molecules in the plasma of the sputtering process,¹⁸ or (2) the widely available nitrogen plasma sources that were traditionally used in radio-frequency molecular beam epitaxy (RF-MBE), and more recently in RF sputtering.¹⁹ The chemical means of achieving high nitrogen reactivity are (1) using other thermochemically unstable molecules, such as ammonia (NH_3), as the nitrogen precursors in metal-organic chemical vapor deposition (MOCVD)²⁰ and tube furnace annealing of metals under the flow of the NH_3 gas; or (2) bulk chemical processes such as reaction with sodium azide (NaN_3) or ion exchange between Na-containing

nitrides and metal halides.²¹ For the sake of brevity of this review, the reader is referred to other reviews^{9,21,22} and handbooks²³ for more information about each of the physical or chemical synthesis methods.

Overall, the theoretical and experimental considerations associated with the stability of the nitrides (Fig. 3-5) illustrate the peculiarity of working with materials away from equilibrium - another Grand Challenge in basic energy science¹¹ that remains to be addressed.²⁴ By extension, the design of metastable nitride materials, both experimentally and computationally, is an important emerging topic in basic energy science. Next, this review article discusses prior experimental and theoretical efforts in this area for the binary nitride materials, both stable (e.g. Ta₃N₅, GaN) and metastable (e.g. Cu₃N, Sn₃N₄).

3. Binary Nitrides

3.1 Copper nitride^{19,25,29}

Copper nitride (Cu₃N) is an interesting material because it is expected to have a defect-tolerant electronic structure. Defect tolerance is a tendency of a semiconductor to maintain its properties despite the presence of crystallographic defects, which results from the antibonding character of the valence band maximum (Fig. 6). In the conventional semiconductors with bonding VBM, the energy levels of the constituent elements are above VBM and below CBM of the resulting compound; so once the atomic bonds are broken defect states appear in the band gap. In contrast, in defect-tolerant semiconductors, the energy levels of the constituent elements and the resulting energy levels of the defect states in the compound, both fall within the bands and lead to shallow states near the band edges, instead of deep defect states in the gap. This defect tolerance hypothesis has been theoretically supported by comparing the results of Cu₃N bulk defect and surface calculations with those of GaN.²⁵ The resulting minimal scattering of electrons and holes should be favorable for the larger-scale device fabrication needed for

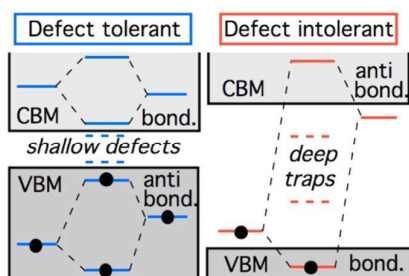


Fig. 6. Electronic structure of defect-tolerant semiconductor with antibonding valence band maximum (VBM), compared to the more common defect-intolerant electronic structure with bonding character of the VBM. Reprinted with permission from Ref.25. Copyright 2014 American Chemical Society

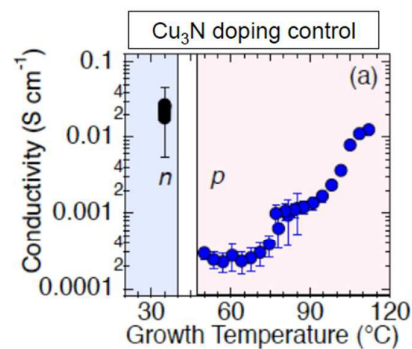


Fig. 7. Conductivity of sputtered Cu₃N, showing transition from *n*-type to *p*-type as the substrate temperature increases.²⁹

solar energy conversion applications to become ubiquitous. In addition to Cu(I) compounds with full *d*¹⁰ closed-shell electronic configuration, this unusual electronic structure is expected to occur in materials that contain other low-valent elements with *s*²*p*⁰ electronic configuration, such as Sn(II), Sb(III), In(I), and Pb(II), such as in the case of CH₃NH₃PbI₃ hybrid perovskites.²⁶

Experimentally, the defect tolerance in Cu₃N manifests itself most prominently in facile bipolar doping, which is quite uncommon for compound semiconductors used for PV or PEC applications. It is known that Cu(I)-based materials often tend to be *p*-type (e.g., CIGS, CZTS) due to abundant copper vacancies,²⁷ whereas nitrides are commonly *n*-type (e.g., GaN, InN) due to oxygen substitutions.²⁸ The Cu₃N seems to inherit the “best of both worlds” and can be doped intrinsically both *p*-type and *n*-type, depending on the growth conditions (Fig. 7). Initially,²⁵ bipolar doping up to 10¹⁶–10¹⁷ cm⁻³ has been measured by Hall effect and confirmed by Seebeck effect in sputtered Cu₃N thin films with 0.1–10.0 cm²/Vs Hall mobility.²⁹ Subsequently, these results have been confirmed by another group using MBE³⁰ and explained in terms of the thermodynamic/kinetic model of defect formation.²⁹ These research results position Cu₃N for future semiconductor device integration—in particular, into devices based on *p*-*n* homojunctions. Solar energy conversion applications of the binary Cu₃N may be limited by its indirect bandgap (1.0 eV) below the optical absorption onset (1.4 eV). However, Cu₃N may still be useful for other optoelectronic applications, where the quantum efficiency rather than the energy conversion efficiency is needed, such as photo-detectors. Also, more favorable optical properties with the same defect-tolerant electronic structure are expected from ternary copper nitrides discussed later on in this article.

The extent and the limits of defect tolerance in copper nitrides can be understood by considering other non-nitride Cu(I)-based compounds. In addition to Cu₃N, other material examples that should have antibonding valence band maxima are Cu(In,Ga)Se₂ (CIGS) and Cu₂ZnSn(S,Se)₄ (CZTS) PV absorbers. Indeed, the CIGS can have ~20% efficiency³¹ despite large off-stoichiometry and polycrystalline morphology,

consistent with the defect tolerance design principle (Fig. 6). However, not as favorable performance of CTZS (~10% efficiency) indicates that the antibonding valence band maximum is a good starting point, but not a sufficient criterion for achieving high solar cell efficiencies. It is not surprising, because “defect tolerance”²⁵ addresses the activation energies (i.e. transition levels) but not concentrations of defects or other possible imperfections (extrinsic contamination, cation disorder).³² In addition, the initially proposed simple defect-tolerance design principle (Fig. 6) is more suitable for valence-band-like defects (acceptors) than for conduction-band-like defects (donors). To address this valence/conduction band issue, the defect-tolerance design principle has recently been extended theoretically to conduction-band-related defects in inorganic semiconductors related to methylammonium (MA) lead halide perovskite MAPbI₃.³³ This extension also theoretically supports broader applicability of the defect-tolerance design principle learned from Cu(I)-based materials, across a wide range of materials chemistries of interest for semiconductor applications (e.g. low-valent Sn, Sb, Pb, Bi, In etc with s^2p^0 electronic configuration).

3.2 Tantalum nitrides

Another class of binary nitrides for solar energy conversion is based on the early transition metal elements. These nitrides have the empty d^0 closed-shell electronic configuration rather than the full d^{10} configuration discussed above for Cu₃N, or the empty p^0 configuration discussed below for Sn₃N₄ and GaN. In the d^0 compounds, the conduction band is derived from the empty d -states of the early transition metal ions, whereas the valence band is predominantly composed of the occupied anion p -orbitals. Thus, as the anion changes from O through mixed O/N all the way to N, the absolute energy of the valence band increases and the bandgap decreases, as illustrated in Fig. 8 based on photoemission measurements of the Ta-based

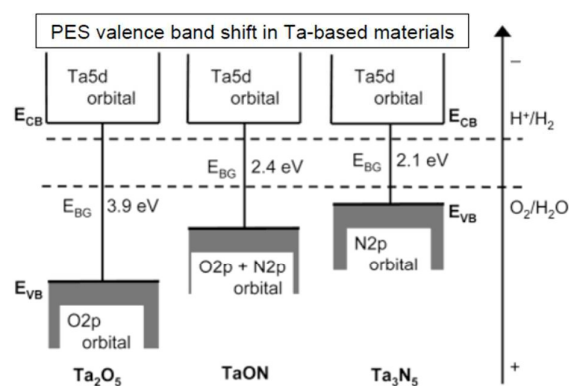


Fig. 8. The progression of the valence band positions of the tantalum oxynitrides measured by photoemission, with respect to water oxidation and hydrogen reduction potentials. As the function of nitrogen increases, the absolute energy of the valence band increases, consistent with Fig. 1. Reprinted with permission from Ref.34. Copyright 2014 American Chemical Society

materials.³⁴ This increase in the valence band position leads to larger band curvature, lower effective masses, and lower band gaps, all of which are favorable for solar energy conversion applications. Indeed, Ta₂O₅, TaON, and Ta₃N₅ have been previously demonstrated in PEC solar cells.³⁵ Recently, a related NbON material has also been studied for these applications.³⁶

Ta₃N₅ and TaON are perhaps the most widely studied d^0 nitrides for PEC fuel generation from sunlight. The initial demonstration of the photoelectrocatalytic activity in TaON and Ta₃N₅³⁷ has been followed by the reports on 3–4 mA/cm² photocurrent from Ta₃N₅ thin films in Fe(CN)₆³⁻/Fe(CN)₆⁴⁻ aqueous solutions and 1–2 mA/cm² photocurrent from the Ta₃N₅ nanowires with catalysts on them used for water splitting.³⁸ Combined theoretical and experimental studies agree that Ta₃N₅ optical absorption onset is at 2.1 eV, and that the indirect gap is 0.2–0.3 eV lower,³⁹ which can be modified by resonant optical absorption.⁴⁰ The same theoretical calculations also suggest relatively heavy and anisotropic hole effective masses, which is consistent with the prior experiments.⁴¹ However, the electron mobility of epitaxial TaON films is quite high: 17 cm²/Vs for the 3.5x10¹⁹ electron concentration.⁴² The Ta₃N₅ is also an n -type semiconductor with carrier concentrations in the 10¹⁶–10²⁰ range depending on the processing conditions.⁴³

3.3 Tin nitride and related materials⁴⁶

Despite the wide use of Si₃N₄ and related materials as dielectrics in the semiconductor industry, the semiconducting properties of other binary group-IV nitrides are relatively unexplored. It is quite surprising, considering the extensive scientific and technological attention to III-nitrides, their nearest neighbors in the periodic table. For example, the few available papers on spinel Sn₃N₄ disagree widely on its bandgap value, with reports ranging from 1.50–2.25 eV (experiment)⁴⁴ and 1.15–1.55 eV (theory).⁴⁵ Our recent experimental/theoretical study⁴⁶ places the Sn₃N₄ bandgap at 1.55 eV, consistent with the other combined study.⁴⁵ In addition, the valence band of Sn₃N₄ was determined to be 6.5 eV below the vacuum level, making this metastable material promising for the water-splitting applications. The sputtered Sn₃N₄ thin films are n -type with the electron concentration of $n = 10^{18}$ cm⁻³ (mobility of $\mu = 1$ cm²/Vs), which is lower than the previously reported values of $n = 10^{20}$ cm⁻³ ($\mu = 3$ cm²/Vs),⁴⁴ making it suitable for the water oxidation part of the water splitting reaction. Unfortunately, theoretical calculation indicated large effective mass ($m_h = 12.9 m_0$) of the valence band, which explains the relatively short 50-nm diffusion length of holes in this material estimated from PEC measurements.

One way to address the heavy hole problem in γ -Sn₃N₄ (spinel) is by alloying with other group-IV metal nitrides. The results of GW theoretical calculation (Table 1) indicate that: (i) alloying Sn₃N₄ in the γ -polymorph spinel structure with other group-IV elements should lower the hole effective masses by 25%–70% and increase the bandgap by 2.0–3.5 eV, while

Table 1. Summary of calculated electronic structure parameters and thermodynamic stability of IV_3N_4 materials in the three known structural polymorphs. Reproduced from Ref.46 with permission from the Royal Society of Chemistry.

Property	α	β	γ
Hole mass (m_0)			
Si_3N_4	2.47	1.47	4.11
Ge_3N_4	2.44	3.90	9.31
Sn_3N_4	2.55	3.46	12.9
Electron mass (m_0)			
Si_3N_4	1.00	0.76	0.52
Ge_3N_4	0.30	0.28	0.54
Sn_3N_4	0.19	0.17	0.18
Band gap (direct gap) (eV)			
Si_3N_4	6.77 (6.85)	6.46 (6.70)	5.09 (5.16)
Ge_3N_4	4.36 (4.41)	4.25 (d)	3.50 (3.52)
Sn_3N_4	1.53 (d)	1.34 (d)	1.54 (d)
Enthalpy of formation (eV per formula unit)			
Si_3N_4	-8.22	-8.22	-7.21
Ge_3N_4	-1.04	-1.02	-0.29
Sn_3N_4	2.31	2.31	1.56

increasing by 3x the electron effective masses; and (ii) stabilizing the α - or β -polymorphs of Sn_3N_4 should bring the hole effective mass down by a factor of 4–5 without significantly changing the electron effective mass or the bandgap. These results suggest that this relatively unexplored family of group-IV nitrides and the related isovalent alloys are promising for PEC solar cells and other optoelectronic applications. Indeed, recent theoretical calculations combined with high-pressure synthesis and synchrotron characterization experiments conclude that the electronic structure of spinel-type Si_3N_4 , Ge_3N_4 , and Sn_3N_4 compounds is attractive for LED applications due to a combination of tunable bandgaps and larger exciton binding energies.⁴⁵

The Sn_3N_4 discussed above is a Sn(IV) nitride, but it is known that Sn can assume IV and II valence states in semiconductor materials. Although the low-valent Sn(II) and mixed-valent Sn(II/IV) binary oxides and chalcogenides are currently widely studied for solar absorber⁴⁷ and transparent electronic⁴⁸ applications based on their favorable properties, even the crystal structures of binary Sn(II) or Sn(II/IV) nitrides have yet to be reported. This is unfortunate because the low-valent Sn(II) containing nitride binaries are expected to have very attractive defect-tolerance properties.^{25,33} However, note that a ternary NaSnN compound with formally divalent Sn(II) has been reported by reaction of intermetallic NaSn with NH_3 ,⁴⁹ suggesting that low-valent Sn nitrides should be possible to synthesize. Thus, more experimental research is needed toward synthesis and structure determination of the binary low-valent Sn_3N_2 and other Sn(II)-containing nitride materials.

3.4 Gallium nitride and related alloys

Gallium nitride (GaN), as well as the related III-nitride materials (AlN , InN) and alloys ($\text{Al}_x\text{Ga}_{1-x}\text{N}$, $\text{In}_x\text{Ga}_{1-x}\text{N}$), are

perhaps the most technologically relevant nitride semiconductors. These materials and alloys are widely used in high electron mobility transistors (HEMTs)⁸ and light-emitting diodes (LEDs).⁷ In addition, GaN can be used in photodetectors,⁵⁰ but its band gap is too wide to efficiently absorb most of the sunlight for photovoltaic applications. To address this issue, $\text{In}_x\text{Ga}_{1-x}\text{N}$ alloys have been proposed as full-spectrum absorbers for radiation-hard photovoltaic solar cells.⁵¹ Initial devices had relatively low quantum efficiency (<60%) attributed in part to InN phase segregation,⁵² but subsequent devices significantly improved this metric.⁵³ These initial successes were followed by a number of studies on GaN-based photovoltaics in thin-film,⁵⁴ multiple quantum well (MQW),⁵⁵ and nanowire⁵⁶ configurations. All these studies led to encouraging reports of 3% and 6%, solar energy conversion efficiency in $\text{In}_x\text{Ga}_{1-x}\text{N}$ MQW heterojunction PV devices with GaN contacts;⁵⁷ however the $\text{In}_x\text{Ga}_{1-x}\text{N}$ homojunction device efficiencies are still much lower.⁵⁸ The performance summary tables of the homojunction and heterojunction $\text{In}_x\text{Ga}_{1-x}\text{N}$ PV devices are provided in Ref. 59. Note that no other nitride semiconductors besides III-nitrides had any PV device performance metrics reported so far.

The GaN and $\text{In}_x\text{Ga}_{1-x}\text{N}$ alloys have been also used for photoelectrochemical water splitting. The early reports on PEC cells with the MOCVD-grown n -type GaN and p -type GaN and Pt counter electrodes,⁶⁰ were soon supported by the comparative studies and the $\text{In}_x\text{Ga}_{1-x}\text{N}$ testing,⁶¹ resulting in H_2 generation at zero bias in the GaN PEC solar cells with 0.6

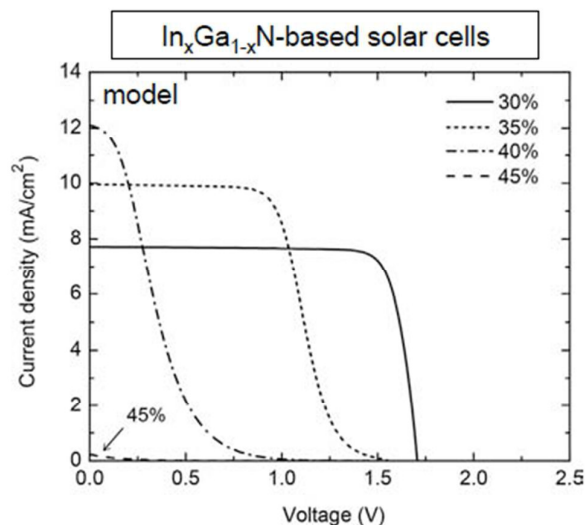


Fig. 9. Modeled n -GaN/ $\text{In}_x\text{Ga}_{1-x}\text{N}/p$ - $\text{In}_{0.25}\text{Ga}_{0.75}\text{N}$ solar cell current density-voltage (J-V) curves as a function of In content in the $\text{In}_x\text{Ga}_{1-x}\text{N}$ layer, showing how the increased polarization mismatch reduces solar cell efficiency.⁶⁹ On the other hand, the modeled J-V curves for $\text{In}_x\text{Ga}_{1-x}\text{N}/\text{GaN}$ solar cells grown on the N-polar GaN surface (not shown in figure) have exactly the same efficiency as without the interface charges.⁶⁸ Reprinted from Ref.69 with permission from Elsevier.

mA/cm^2 current.⁶² This work was followed by several other PEC studies on $\text{In}_x\text{Ga}_{1-x}\text{N}$,⁶³ culminating in 2.9% solar-to-electricity and 1.5% solar-to-fuel conversion efficiency in $\text{In}_x\text{Ga}_{1-x}\text{N}/\text{GaN}$ MQW devices under AM1.5 illumination and zero bias.⁶⁴ In parallel, nanostructured GaN and $\text{In}_x\text{Ga}_{1-x}\text{N}$ photoelectrodes have achieved current densities of 2-4 mA/cm^2 and incident photon-to-current efficiencies of 15-30% in recent years,⁶⁵ resulting into the solar-to-fuels conversion efficiencies of $\sim 1.8\%$ under concentrated sunlight.⁶⁶

Besides the growth-related challenges of the $\text{In}_x\text{Ga}_{1-x}\text{N}$ system (GaN/InN phase separation, structural defects), another complicating factor for PV and PEC solar cell fabrication is the non-centrosymmetric character of the wurtzite structure. The lack of inversion symmetry in wurtzite materials leads to spontaneous- and strain-induced piezoelectric polarization, well-known in GaN-based materials used for LEDs and HEMTs. In fact, the two-dimensional electron gas (2DEG) that results from the polarization is the key enabling feature for GaN application in radio-frequency HEMTs;⁸ however, the related quantum-confined Stark effect (QCSE) in GaN-based multiple quantum wells is detrimental to blue- and white LED performance.⁶⁷ In the case of PV (Fig. 9), drift-diffusion modeling determined that polarization mismatch charges at the interface between the lower-gap $\text{In}_x\text{Ga}_{1-x}\text{N}$ absorber and the wider-gap *n*-type Ga-polar GaN substrate may lead to drift of the photoexcited charge carriers in the direction opposite to the contact polarity, which reduces the energy conversion efficiency of the photovoltaic solar cells (not the case for N-polar surfaces)^{68,69} These challenges may be addressed by the $\text{In}_x\text{Ga}_{1-x}\text{N}$ *p-i-n* homojunction device architecture,⁶⁹ or by growth of $\text{In}_x\text{Ga}_{1-x}\text{N}$ on non-polar, semi-polar GaN surfaces, as recently discussed for GaN LEDs.⁷⁰ The polarization effects are also likely to be important for the performance of the photoelectrochemical solar cells.

An alternative way to improve the sunlight absorption of GaN, is by *homostructural/heterovalent* alloying, such as in $(\text{Ga}_{1-x}\text{Zn}_x)(\text{N}_{1-x}\text{O}_x)$.⁷¹ These (Ga,Zn)(O,N) alloys are different than the traditional *homostructural/homovalent* $\text{In}_x\text{Ga}_{1-x}\text{N}$ alloys, in that both end-point materials (GaN and ZnO) do not absorb the light, whereas the ZnO:GaN alloy does. Yet another way to tune the physical properties of III-nitrides is through *heterostructural/heterovalent* alloying, such as in the case of (Al,Sc)N studied for piezoelectric applications.⁷² The successful synthesis of these unusual alloys has been demonstrated,⁷³ but the ScN bandgap is too wide for efficient solar absorption. Therefore, alloying of GaN or InN with other narrow-gap main-group (YN, LaN) or transition metal (CrN, MnN, FeN) rocksalt nitrides may be promising. We also note that such heterostructural/heterovalent alloying has been successfully demonstrated for tuning the optical absorption and electrical transport properties in wurtzite $\text{Mn}_{1-x}\text{Zn}_x\text{O}$ alloys for PEC water splitting.⁷⁴

4. Ternary nitrides

4.1 Wurtzite-related structures⁷⁷

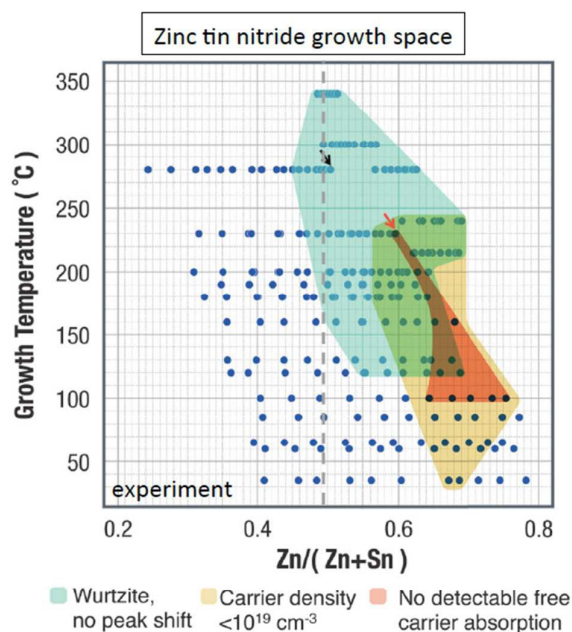


Fig. 10. Composition-Temperature growth phase space of zinc tin nitride, showing that the wurtzite material with low carrier density can be obtained at Zn-rich synthesis conditions. The red and the black arrows refer to the observed orthorhombic ordered phase and the lowest electron concentration, respectively. Reproduced from Ref.77 with permission from the Royal Society of Chemistry.

The II-IV- N_2 nitrides are a class of semiconductor materials related to the wurtzite III-N nitrides. In these ternary II-IV- V_2 compounds, the wurtzite III-V unit cell is doubled, and two group-III elements are replaced by a group-II element and a group-IV element. The resulting crystal structure is also related to the hexagonal wurtzite, but it may have II/IV cation ordering, giving rise to a lower-symmetry orthorhombic unit cell. Similar to the (Al,Ga,In)N material system, the $\text{Zn}(\text{Sn,Ge,Si})\text{N}_2$ material system provides bandgap tuning in a wider range from >5 eV to <1 eV, which covers most of the solar spectrum and extends into the ultraviolet range.⁷⁵ As such, these II/IV-nitride materials may have similar promise as the III-nitride alloys for solar cell PV and full-spectrum LED applications, without necessarily having the problems related to the group-III element miscibility in the alloys. However, the synthesis of the light-absorbing semiconductor-quality ZnSnN_2 material is quite challenging due to degenerate electron concentration ($\sim 10^{20} \text{ cm}^{-3}$) attributed to unintentional oxygen incorporation and other defects in the material.⁷⁶

Very recently, we demonstrate *n*-type doping control in zinc tin nitride using high-throughput experimental approach, including combinatorial synthesis and spatially resolved characterization.⁷⁷ We found that the carrier concentration can be reduced by synthesizing the thin films at Zn-rich conditions and relatively low substrate temperatures, where such off-stoichiometry is possible without structural phase separation (Fig. 10). The resulting zinc tin nitride films have

electron concentration of 10^{18} cm^{-3} with mobility of $8 \text{ cm}^2/\text{Vs}$ at the composition of $\text{Zn}/(\text{Zn} + \text{Sn}) = 0.60$ and substrate growth temperature of 230°C . This relatively low doping level let us avoid the Burstein–Moss shift and free-carrier absorption effects, so we could accurately determine the theoretically predicted 1.0-eV bandgap of the cation-disordered wurtzite material.⁷⁸ These experiments extend the range of bandgaps available in the II-IV-N₂ materials system to the near-infrared part of the spectrum. Note that this $\text{Zn}_{1-x}\text{Sn}_x\text{N}_2$ wurtzite material has no well-defined Zn and Sn sites on the cation sublattice, which can also be thought of as a very high concentration of the cation antisite defects.

The 1–2-eV bandgap tuning depending on the degree of cation disorder at the ZnSnN_2 stoichiometry ($\text{Zn}:\text{Sn}=1:1$) is a useful optical absorption property of this material.^{78,79} This is because the band gap tuning can be achieved at the fixed lattice constant (without changing the composition), just by changing the growth temperature that controls the cation disorder. However, such cation disorder may also have undesired consequences for the electrical charge-transport properties. Preliminary experimental estimations of electron effective mass (m^*) in the wurtzite zinc tin nitride⁷⁷ indicate that the m^* is higher ($\sim 0.5 m_e$) than the theoretically predicted value for the both fully-random wurtzite structure and fully-ordered orthorhombic structure (both $\sim 0.1 m_e$),⁷⁹ which may be related to the non-random cation disorder. Note that the Zn/Sn ordering on the wurtzite cation sublattice and the resulting orthorhombic ZnSnN_2 crystal structure is similar to the Cu/Zn/Sn ordering on the zincblende cation sublattice and the resulting “kesterite” tetragonal $\text{Cu}_2\text{ZnSnS}_4$ (CZTS) crystal structure.⁸⁰ The effects of the non-random Cu/Zn cation disorder and the resulting potential fluctuations in covalent

CZTS on electrical charge transport of photoexcited electrons have been discussed extensively in recent literature.³² Similar effects are in principle possible but not necessary in the more ionic zinc tin nitride, so more research is needed to address this point.

4.2 Delafossites^{83,84}

An emerging family of ternary nitrides crystallizes in the layered delafossite crystal structure and includes materials such as CuTaN_2 and CuNbN_2 . The delafossite structure is well known in the field of *p*-type transparent conducting oxides (TCOs), because the archetype material CuAlO_2 ⁸¹ is a delafossite. The archetype nitride delafossite CuTaN_2 was first synthesized a long time ago in bulk form using ion exchange,⁸² but its properties were unknown, like many other nitrides available in ICSD. More recently,⁸³ it was shown that despite its positive theoretical heat of decomposition ($+0.11 \text{ eV/at}$ with respect to N_2 , Cu and Ta_3N_5), CuTaN_2 is experimentally stable *in air* up to 250°C . Theoretical calculations and experimental measurements agree that CuTaN_2 has a strong optical absorption onset in 1.4–1.5 eV range, just above its calculated 1.3-eV lowest-energy indirect bandgap (Fig. 11). The calculations also indicate that the absorption coefficient of CuTaN_2 is very large ($>10^5 \text{ cm}^{-1}$ above 1.5 eV), suggesting it is suitable for solar energy conversion technologies where ultrathin absorber layers are necessary, such as dye-sensitized or drift-enhanced solar cells.

In contrast to CuTaN_2 , the crystal structure of the related CuNbN_2 material has not been reported until very recently.⁸⁴ The reason is that the ion-exchange synthesis of CuNbN_2 is more challenging, resulting in a trace amount of NbN impurities; however recently the crystal structure of CuNbN_2 has been determined and refined to be the delafossite.⁸⁴ The CuNbN_2 properties are also unique—the in-plane (m_{in}) and out-of-plane (m_{out}) effective masses of electrons and holes in CuNbN_2 are quite isotropic ($m_{out}/m_{in} = 1.3 - 2.1$) and low ($m^* = 0.3 - 0.7 m_0$), despite the layered crystal structure. These good semiconducting properties combined with the anisotropic crystal structure also make the nitride delafossites attractive for other applications, such as thermoelectrics.⁸⁵ Compared to CuTaN_2 , the bandgap of CuNbN_2 is lower and more indirect ($E_{dir} = 1.3\text{--}1.4 \text{ eV}$, $E_{ind} = 0.9 \text{ eV}$). Based on these results, bandgap-tunable $\text{Cu}(\text{Nb,Ta})\text{N}_2$ absorbers can be envisioned in the future,⁸⁴ which would require thin film growth. This may be accomplished using the current knowledge about the bulk material’s synthesis routes (ion exchange), but in a thin film form.

4.3 Theoretical predictions⁸⁴

It is quite surprising that besides the aforementioned copper-based nitride delafossites, and three materials from the Cu-Ae-N (Ae = Ca, Sr, and Ba) family,⁸⁶ no other closed-shell ternary copper nitrides have been reported. This is not necessarily expected, given the large number of studied ternary copper oxides, chalcogenides, and mixed-anion compound studied for PV absorbers and contacts.⁸⁷ To shed

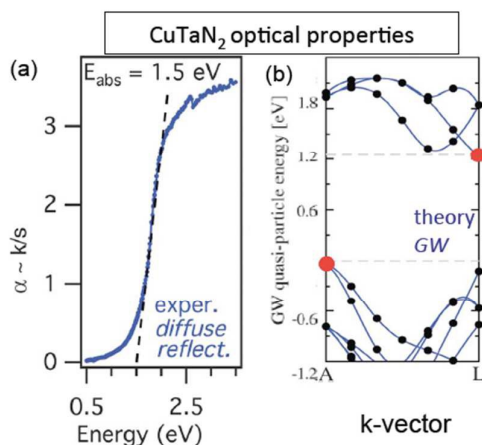


Fig. 11 (a) Experimentally measured optical absorption spectra of CuTaN_2 powders synthesized by ion exchange approach, showing strong onset of optical absorption at $\sim 1.5 \text{ eV}$. (b) Theoretically calculated band structure of CuTaN_2 along a high symmetry direction, revealing its slightly indirect 1.3 eV band gap and disperse band edges. Reproduced from Ref.83 with permission from the Royal Society of Chemistry.

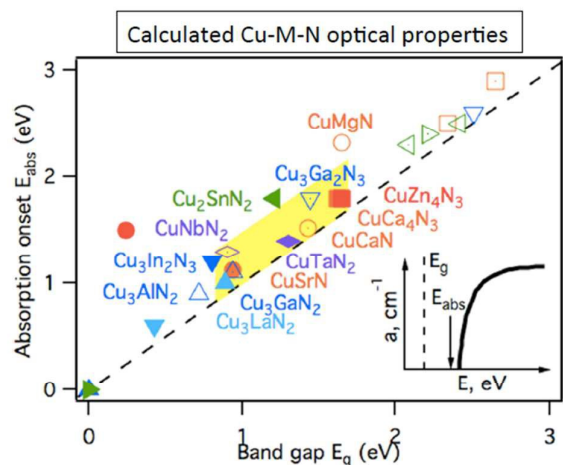


Fig. 12. Calculated optical properties of Cu-M-N compounds (E_g and E_{abs}), showing the compositions of materials suitable for solar energy conversion applications (yellow region). Reprinted with permission from Ref. 84. Copyright 2014 American Chemical Society.

more light onto this chemical asymmetry, thermodynamic stabilities of 44 previously unreported ternary copper nitrides have been examined using the structure-prototyping approach,⁸⁸ and optoelectronic properties of a subset of 18 materials have been calculated using the GW method.⁸⁴ The results of these calculations indicate that many of these ternary copper nitrides are metastable, just like the previously synthesized CuTaN_2 and CuNbN_2 . Several of these predicted nitrides, such as $\text{Cu}_3\text{Ga}_2\text{N}_3$ and $\text{Cu}_3\text{In}_2\text{N}_3$, have suitable optical absorption and effective mass properties for future solar energy conversion applications (Fig. 12). These results call for more intense experimental attempts to synthesize the novel metastable materials of interest, using the synthesis approaches discussed in the methods section (Fig. 4, Fig. 5).

Going beyond the ternary copper nitrides, another first-principles computational study focused on high-throughput screening of a wide range of possible nitride and oxynitrides for water-splitting photocatalysts, based on the structure-prediction approach using ionic substitution.⁸⁹ A few thousands of the ICSD-reported and theoretically constructed materials have been calculated for their phase stability and physical properties related to photocatalytic applications, such as band edge positions and bandgaps. The results of this high-throughput search reproduced the previously known nitride-based photocatalysts, including binary (Ta_3N_5), ternary (TaON), and multinary (LaTiO_2N , $\text{Ba}_2\text{TaO}_2\text{N}$) materials.³⁵ These results also suggested a few previously unrecognized materials for this application ($\text{Ti}_3\text{O}_3\text{N}_2$, $\text{La}_2\text{TiO}_2\text{N}_2$). Besides the stoichiometric compounds, solid solutions of $\text{Ba}_2\text{TaO}_3\text{N}$, $\text{Sr}_2\text{NbO}_3\text{N}$, and $\text{La}_2\text{TiO}_2\text{N}_2$ in their same Sr_2SnO_4 -type crystal structure may also be suitable water-splitting materials.

4.4 Perovskites

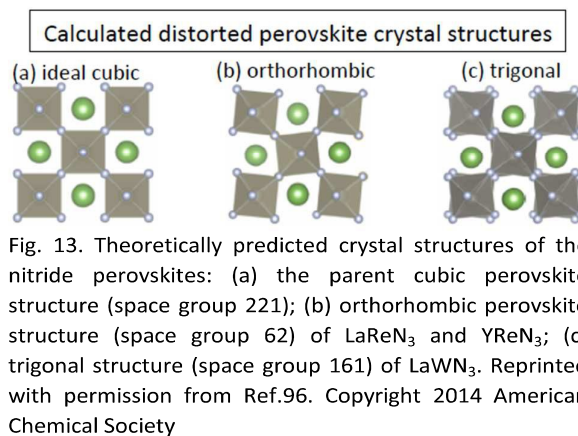


Fig. 13. Theoretically predicted crystal structures of the nitride perovskites: (a) the parent cubic perovskite structure (space group 221); (b) orthorhombic perovskite structure (space group 62) of LaReN_3 and YReN_3 ; (c) trigonal structure (space group 161) of LaWN_3 . Reprinted with permission from Ref.96. Copyright 2014 American Chemical Society

Perovskites with the general formula ABX_3 are a very large structural class of materials with diverse properties.⁹⁰ Oxide-based perovskites have broad commercial applications in ferroelectric capacitors (e.g., BaTiO_3), piezoelectric elements (e.g., PbTiO_3), and non-linear optics (e.g., LiNbO_3),⁹¹ and have been studied for solar energy conversion (e.g., BiFeO_3 ,⁹² $\text{Bi}_2\text{FeCrO}_6$).⁹³ In the solar energy conversion field, hybrid organic-inorganic halide perovskites such as $\text{CH}_3\text{NH}_3\text{PbI}_3$ ⁹⁴ have recently attracted tremendous attention due to the rapid rise in their energy conversion efficiencies. Nevertheless, very few nitride perovskites are known, limited to exotic metal chemistries such as TaThN_3 .⁹⁵ Recently, several more perovskite-related nitrides were predicted theoretically,⁹⁶ including LaReN_3 , YReN_3 , and LaWN_3 (Fig. 13). The high oxidation states of metals in all these materials illustrate the challenge with the perovskite nitrides: the total valence of nine between the A and B metals in the perovskite is required for the charge balance with three trivalent nitrogen ions in the ABN_3 perovskite structure. The problem is that there are not many metals that can assume such high valence states.

However, one of the predicted materials, LaWN_3 , has been synthesized in the past,⁹⁷ but containing 20% oxygen ($\text{LaWO}_{0.6}\text{N}_{2.4}$). This hints to a possible route to address the nitride perovskite challenge—specifically, that the oxynitride perovskites may be easier to synthesize. Indeed, many more oxynitride perovskites are known, and some of them are actively used for inorganic pigment applications.⁹⁸ Their pigment use suggests reasonable light-absorbing properties of the oxynitride perovskites, in the context of their solar energy conversion applications. Recently, 5,400 known oxide- and oxynitride perovskite materials have been computationally screened for photocatalysis, and four promising oxynitride candidates were identified.⁹⁹ Indeed, these BaTaO_2N , CaTaO_2N , SrTaO_2N , and LaTiO_2N materials had been actively studied experimentally for PEC applications in the past,³⁵ and pointed out by the other aforementioned high-throughput theoretical study.⁸⁹ According to neutron diffraction, the oxynitride perovskite materials have very well-ordered O and N on the anion sublattice,¹⁰⁰ indicating that the ionic charge difference is an important criterion for anion ordering of the elements with similar ionic radii.

Summary and Conclusions

The two important future directions in design of novel semiconducting nitrides for solar energy conversion are (1) development of nitride-based PV and PEC devices, and (2) research related to discovering more new nitride materials. Some challenges and opportunities of these two directions are highlighted next.

(1) First, *device development* of PV and PEC solar cells and other optoelectronic devices is necessary to build upon the promise of these novel nitride materials for solar energy conversion applications. Note that so far none of the novel nitrides discussed above (except for GaN-related materials) has been integrated into a PV device, but some PEC testing has been performed. For the PV device development, doping and electrical transport of the resulting *majority* charge carriers have to be controlled first, in order to form a rectifying *p-n* junction. The currently achievable carrier densities and the corresponding mobilities are summarized in Table 2 for several novel semiconductor nitrides discussed in this review. In longer term, the recombination and transport of the *minority* charge carriers excited by the incident light are even more important for the solar energy conversion efficiency; yet much less is known about these photexcited charge carrier properties in the novel nitride semiconductors. In addition to the bulk minority carrier lifetime and diffusion/drift lengths, the extraction and injection of the minority charge carriers through the electrical contacts should be addressed, including band offsets, interface trap states, surface oxide passivation and other interfacial phenomena. Fortunately, there are many valuable insights that can be gained in this regard from researchers working on GaN LEDs, HEMTs, and other electronic devices based on III-nitride semiconductors.

(2) Second, more of the basic *materials research* is needed, so to further expand the range of available nitride materials, and to better understand and control their optoelectronic properties. The former need, including materials synthesis and structure prediction challenges, can significantly benefit from tight integration of experiments and computations akin to that in the aforementioned materials-by-design approaches. However, the latter need may also require better insights into the effects of ionicity, or even polarity, on the optoelectronic processes in semiconductors. Here, the input from the researchers working on traditional III-nitrides (e.g. GaN) and polar electronic oxides (e.g. SrTiO₃) would also be desired.

Thus it appears that both future research directions highlighted here would require more interactions between scientists working on basic research of nitride materials discovery such as those summarized in Table 2, and researchers focused on applied development of well-established nitride semiconductors such as GaN. On one hand, the scientists working on novel nitrides should not shy away from the device development opportunities, or at least the lessons learned from the established III-nitrides. Demonstration of hydrogen-assisted dopant activation, template layers for seeded growth of foreign substrates, double heterostructures, and quantum wells are just a few

Table 2. Summary of concentrations and mobilities of majority charge carriers in selected novel nitride semiconductors measured using Hall effect, except for the NbON where Mott-Schottky analysis was used. Measured optical band gaps are also provided. Note that among all the materials, only Cu₃N has been reported to be *p*-type dopable like GaN; all other nitrides are *n*-type

Material	E_g , eV	c , cm ⁻³	μ , cm ² /Vs	Reference
<i>p</i> -Cu ₃ N	1.0	10 ¹⁶ -10 ²⁰	10-0.1	25, 30
Cu ₃ N	1.0	10 ¹⁷ -10 ²⁰	0.1	25, 30
Sn ₃ N ₄	1.6	10 ¹⁸ -10 ²⁰	1-3	46, 44
TaON	2.3	3.5x10 ¹⁹	17	36
NbON	2.1	3.5x10 ²⁰	-	42
Ta ₃ N ₅	2.1	10 ¹⁶ -10 ²⁰	4-1	43
ZnSnN ₂	1.0	10 ¹⁸ -10 ²⁰	1-8	77

examples of device-engineering related but materials-science rich problems in GaN;⁷ implementation of similar ideas in novel nitrides is needed. On the other hand, the researchers working on the well-established III-nitrides should not be afraid to take a full advantage of the continuously growing list of novel nitride semiconductors for implementation of optoelectronic devices (Table 2). Often, such novel nitride experiments or calculations are, in fact, not any more difficult than the corresponding III-nitride research. Yet the impact of introducing an entirely new nitride material to the optoelectronic community could be much larger than studying the previously well-know materials, as proven by the 2014 Nobel Prize in Physics for GaN.

Acknowledgements

The writing of this review article were supported by the U.S. Department of Energy, Office of Science, Basic Energy Sciences, as a part of the DOE Energy Frontier Research Center "Center for Next Generation of Materials by Design: Incorporating Metastability". The author's part of work on the tin nitrides reviewed here were also supported from this funding source. The author's work on the copper nitrides reviewed here was supported by U.S. Department of Energy, Office of Energy Efficiency and Renewable Energy, as a part of the "Ternary Copper Nitride Absorbers" Next Generation PV II project within the SunShot Initiative. The author's part of work on the zinc tin nitride was supported by U.S. Department of Energy, Office of Energy Efficiency and Renewable Energy, as a part of the "Non-Proprietary Partnering Opportunity" project within the SunShot Initiative. All these projects have been performed under DOE Contract No. DE-AC36-08GO28308 to NREL. The author would like to thank A. Tamboli and A. Fioretti for useful feedback on this review paper. Illuminating discussions with A. Holder, S. Lany and G. Ceder about the origins of the nitrides metastability, are gratefully acknowledged.

References

- 1 P.A. Basore, D. Chung, and T. Buonassisi, 42nd IEEE Photovoltaic Specialists Conf., New Orleans, June 2015.
- 2 C. Wadia, A.P. Alivisatos, and D.M. Kammen, *Environmental Science & Technology*, 2009, **43**(6), 2072-2077.
- 3 L. Hultman, *Vacuum* 2000, **57**(1), 1-30.
- 4 J. Robertson and S. J. Clark, *Phys. Rev. B* 2011, **83**, 075205; W. Walukiewicz *Physica B* 2001, **302–303**, 123–134
- 5 S. Rühle, A. Y., Anderson, H. N. Barad, B. Kupfer, Y. Bouhadana, E. Rosh-Hodesh, and A. Zaban, *The Journal of Physical Chemistry Letters*, 2012, **3**(24), 3755-3764.
- 6 C.X Kronawitter, L. Vayssieres, S. Shen, L. Guo, D. A. Wheeler, J. Z. Zhang, J. Z., B. R. Antoun, and S. S. Mao, *Energy & Environmental Science*, 2011 **4**(10), 3889-3899.
- 7 S. Nakamura, *Reviews of Modern Physics*, 2015, **87**(4), 1139; H. Amano, *Reviews of Modern Physics*, 2015, **87**(4), 1133; I. Akasaki, *Reviews of Modern Physics*, 2015, **87**(4), 1119.
- 8 U.K. Mishra, P. Parikh, and Y.-F. Wu, *Proceedings-IEEE*, 2002, **90**(6), 1022-1031.
- 9 D.H. Gregory, *Journal of the Chemical Society, Dalton Transactions*, 1999, **3**, 259-270.
- 10 E. Gregoryanz, C. Sanloup, M. Somayazulu, J. Badro, G. Fiquet, H.-K. Mao, and R.J. Hemley, *Nature Materials*, 2004, **3**(5), 294-297; J.C. Crowhurst, A.F. Goncharov, B. Sadigh, C.L. Evans, P.G. Morrall, J.L. Ferreira, and A.J. Nelson, *Science*, 2006, **311**(5765), 1275-1278.
- 11 "Directing Matter and Energy: Five Challenges for Science and the Imagination." A Report from the Basic Energy Sciences Advisory Committee U.S. DOE (2007); G.R. Fleming and M.A. Ratner, *Physics Today*, 2008, **28**
- 12 Materials Genome Initiative for Global Competitiveness. <https://www.whitehouse.gov/mgi>, June 2011.
- 13 S. Curtarolo, G.L.W. Hart, M. Buongiorno Nardelli, N. Mingo, S. Sanvito, and O. Levy, *Nature Materials*, 2013, **12**(3), 191-201.
- 14 M.L. Green, I. Takeuchi, and J.R. Hatrick-Simpers, *Journal of Applied Physics*, 2013, **113**(23), 231101.
- 15 A. Zakutayev, X. Zhang, A. Nagaraja, L. Yu, S. Lany, T.O. Mason, D.S. Ginley, and A. Zunger, *Journal of the American Chemical Society*, 2013, **135**(27), 10048-10054; R. Gautier, X. Zhang, L. Hu, L. Yu, Y. Lin, T.O.L. Sunde, D. Chon, K.R. Poeppelmeier, and A. Zunger, *Nature Chemistry*, 2015, **7**(4), 308-316.
- 16 P. Zawadzki, L.L. Baranowski, H. Peng, E.S. Toberer, D.S. Ginley, W. Tumas, A. Zakutayev, and S. Lany, *Appl. Phys. Lett.*, 2013, **103**, 253902; A.W. Welch, P.P. Zawadzki, S. Lany, C.A. Wolden, and A. Zakutayev, *Solar Energy Materials and Solar Cells*, 2015, **132**, 499-506.
- 17 A.W. Welch, L.L. Baranowski, P. Zawadzki, S. Lany, C.A. Wolden, and A. Zakutayev, *Appl. Phys. Exp.*, 2015, **8**, 082301; A.W. Welch, L.L. Baranowski, P. Zawadzki, C. DeHart, S. Johnston, S. Lany, C.A. Wolden, and A. Zakutayev, arXiv preprint arXiv:1504.01345 (2015).
- 18 S. C. D. S. PalDey, and S. C. Deevi. *Materials Science and Engineering: A* 2003, **342**(1), 58-79.
- 19 C.M. Caskey, R. Richards, D.S. Ginley, and A. Zakutayev, *Mater. Horiz.*, 2014, **1**, 424.
- 20 D. A. Neumayer, and J. G. Ekerdt., *Chemistry of materials*, 1996, **8**(1), 9-25.
- 21 R. Niewa, and F. J. DiSalvo, *Chemistry of materials*, 1998 **10**, 2733-2752.
- 22 S.C. Jain, M. Willander, J. Narayan, and R. Van Overstraeten, *Journal of Applied Physics*, 2000, **87**(3), 965-1006.
- 23 Morkoç, H. *Handbook of Nitride Semiconductors and Devices, Materials Properties, Physics and Growth*, 2009, John Wiley & Sons.
- 24 "Challenges at the Frontiers of Matter and Energy: Transformative Opportunities for Discovery Science," A Report from the Basic Energy Sciences Advisory Committee U.S. DOE (2015).
- 25 A. Zakutayev, C.M. Caskey, A.N. Fioretti, D.S. Ginley, J. Vidal, V. Stevanovic, E. Tea, and S. Lany, *J. Phys. Chem. Lett.*, 2014, **5**, 1117.
- 26 M. M. Lee, J. Teuscher, T. Miyasaka, T. N. Murakami, and H. J. Snaith, *Science*, 2012, **338**(6107), 643-647.
- 27 J. Pohl and K. Albe, *Journal of Applied Physics*, 2010, **108**(2), 3509.
- 28 G.A. Slack, L.J. Schowalter, D. Morelli, and J.A. Freitas, *Journal of Crystal Growth*, 2002, **246**(3), 287-298.
- 29 A.N. Fioretti, C.P. J. Vinson, D. Nordlund, D. Prendergast, A.C. Tamboli, C.M. Caskey, F. Tuomisto, F. Linez, S.T. Christensen, E.S. Toberer, S. Lany, and A. Zakutayev, private communication
- 30 K. Matsuzaki, T. Okazaki, Y.-S. Lee, H. Hosono, and T. Susaki, *Applied Physics Letters*, 2014, **105**(22), 222102.
- 31 M.A. Green, K. Emery, Y. Hishikawa, W. Warta, and E.D. Dunlop, *Progress in Photovoltaics: Research and Applications*, 2015, **23**(1), 1-9.
- 32 P. Zawadzki, A. Zakutayev, and S. Lany, *Phys. Rev. Appl.*, 2015, **3**, 034007.
- 33 R.E. Brandt, V. Stevanović, D.S. Ginley, and T. Buonassisi, *MRS Communications*, 2015, **5**, 265-275.
- 34 W.-J. Chun, A. Ishikawa, H. Fujisawa, T. Takata, J.N. Kondo, M. Hara, M. Kawai, Y. Matsumoto, and K. Domen, *The Journal of Physical Chemistry*, 2003, **B107**(8), 1798-1803.
- 35 Y. Moriya, T. Takata, and K. Domen, *Coordination Chemistry Reviews*, 2013, **257**(13), 1957-1969.
- 36 R. Kikuchi, T. Kouzaki, T. Kurabuchi, and K. Hato, *Electrochemistry*, 2015, **83**(9), 711-714.

- 37 G. Hitoki, T. Takata, J.N. Kondo, M. Hara, H. Kobayashi, and K. Domen, *Chemical Communications*, 2002, **16**, 1698-1699; G. Hitoki, A. Ishikawa, T. Takata, J.N. Kondo, M. Hara, and K. Domen, *Chemistry Letters*, 2002, **7**, 736-737.
- 38 A. Ishikawa, T. Takata, J.N. Kondo, M. Hara, and K. Domen, *The Journal of Physical Chemistry*, 2004, **B108**(30), 11049-11053; Y. Li, T. Takata, D. Cha, K. Takanahe, T. Minegishi, J. Kubota, and K. Domen, *Advanced Materials*, 2013, **25**(1), 125-131.
- 39 J.M. Morbec, I. Narkeviciute, T.F. Jaramillo, and G. Galli, *Physical Review B*, 2014, **90**(5), 155204.
- 40 A. Dabirian and R. Van de Krol, *Applied Physics Letters*, 2013, **102**(3), 033905.
- 41 B.A. Pinaud, P.C.K. Vesborg, and T.F. Jaramillo, *The Journal of Physical Chemistry C*, 2012, **116**(30), 15918-15924.
- 42 A. Suzuki, Y. Hirose, D. Oka, S. Nakao, T. Fukumura, S. Ishii, K. Sasa, H. Matsuzaki, and T. Hasegawa, *Chemistry of Materials*, 2013, **26**(2), 976-981.
- 43 D. AlvesáSilva, *Physical Chemistry Chemical Physics*, 2015, **17**(4), 2670-2677.
- 44 Y. Inoue, M. Nomiya, and O. Takai, *Vacuum*, 1998, **51**, 673-676; R.G. Gordon, D.M. Hoffman, and U. Riaz, *Chem. Mater.*, 1992, **4**, 68-71.
- 45 T.D. Boyko, A. Hunt, A. Zerr, and A. Moewes, *Phys. Rev. Lett.*, 2013, **111**, 097402; M. Huang and Y.P. Feng, *J. Appl. Phys.*, 2004, **96**, 4015-4017.
- 46 C.M. Caskey, J.A. Seabold, V. Stevanović, M. Ma, W.A. Smith, D.S. Ginley, N.R. Neale, R.M. Richards, S. Lany, and A. Zakutayev, *Journal of Materials Chemistry C*, 2015, **3**(6), 1389-1396.
- 47 V. Steinmann, R. Jaramillo, K. Hartman, R. Chakraborty, R.E. Brandt, J.R. Poindexter, Y.S. Lee et al., *Advanced Materials*, 2014, **26**(44), 7488-7492.
- 48 E. Fortunato, R. Barros, P. Barquinha, V. Figueiredo, S.-H. Ko Park, C.-S. Hwang, and R. Martins, *Appl. Phys. Lett.*, 2010, **97**(5), 052105.
- 49 N.S.P. Watney, Z.A. Gál, M.D.S. Webster, and S.J. Clarke, *Chemical Communications*, 2005, **33**, 4190-4192.
- 50 M.A. Khan, J.N. Kuznia, D.T. Olson, M. Blasingame, and A.R. Bhattarai, *Applied Physics Letters*, 1993, **63**(18), 2455-2456; X. Zhang, P. Kung, D. Walker, J. Piotrowski, A. Rogalski, A. Saxler, and M. Razeghi, *Applied Physics Letters*, 1995, **67**(14), 2028-2030.
- 51 J. Wu, W. Walukiewicz, K.M. Yu, W. Shan, J.W. Ager III, E.E. Haller, H. Lu, W.J. Schaff, W.K. Metzger, and S. Kurtz, *Journal of Applied Physics*, 2003, **94**(10), 6477-6482.
- 52 O. Jani, I. Ferguson, C. Honsberg, and S. Kurtz, *Applied Physics Letters*, 2007, **91**(13), 132117.
- 53 E. Matioli, C. Neufeld, M. Iza, S.C. Cruz, A.A. Al-Heji, X. Chen, R.M. Farrell, et al., *Applied Physics Letters*, 2011, **98**(2), 021102; C.J. Neufeld, N.G. Toledo, S.C. Cruz, M. Iza, S.P. DenBaars, and U.K. Mishra, *Applied Physics Letters*, 2008, **93**(14), 3502.
- 54 X.-M. Cai, S.-W. Zeng, and B.-P. Zhang, *Applied Physics Letters*, 2009, **95**(17), 3504; X. Zheng, R.-H. Horng, D.-S. Wu, M.-T. Chu, W.-Y. Liao, M.-H. Wu, R.-M. Lin, and Y.-C. Lu, *Applied Physics Letters*, 2008, **93**(26), 261108.
- 55 R. Dahal, B. Pantha, J. Li, J. Y. Lin, and H.X. Jiang, *Applied Physics Letters*, 2009, **94**(6), 063505.
- 56 Y. Dong, B. Tian, T.J. Kempa, and C.M. Lieber, *Nano Letters*, 2009, **9**(5), 2183-2187.
- 57 R. Dahal, J. Li, K. Aryal, J. Y. Lin, and H. X. Jiang, *Appl. Phys. Lett* 2010, **97**, 073115.; B. W. Liou, *Thin Solid Films* 2011, **520**, 1084-1090.
- 58 X. M. Cai, S. W. Zeng, and B.P. Zhang, *Applied Physics Letters*, 2009, **95**(17), 3504; A. Yamamoto, M.R. Islam, T.T. Kang, and A. Hashimoto, *physica status solidi (c)*, 2010, **7**(5), 1309-1316.
- 59 A. Bhuiyan, K. Sugita, A. Hashimoto, A. Yamamoto, *IEEE Journal of Photovoltaics*, 2012, **2**(3), 276-293.
- 60 N. Kobayashi, T. Narumi, and R. Morita, *Japanese journal of applied physics*, 2005, **44**(6L), L784; K. Fujii, T. Karasawa, and K. Ohkawa, *Japanese journal of applied physics*, 2005, **44**(4L), L543.
- 61 K. Fujii, K. Kusakabe, and K. Ohkawa, *Japanese journal of applied physics*, 2005, **44**(10R), 7433; K. Fujii, K. Ohkawa, *Japanese journal of applied physics*, 2005, **44**(7L), L909.
- 62 M. Ono, K. Fujii, T. Ito, Y. Iwaki, A. Hirako, T. Yao, and K. Ohkawa, *Journal of Chemical Physics*, 2007, **126**(5), 54708-54708.
- 63 W. Luo, B. Liu, Z. Li, Z. Xie, D. Chen, Z. Zou, and R. Zhang, *Applied Physics Letters*, 2008, **92**, 262110; J. Li, J. Y. Lin, and H. X. Jiang, *Applied Physics Letters*, 2008, **93**, 162107; K. Aryal, B. N. Pantha, J. Li, J. Y. Lin, and H. X. Jiang, *Applied Physics Letters* 2010, **15**, 01017
- 64 R. Dahal, B. N. Pantha, J. Li, J. Y. Lin, and H. X. Jiang, *Applied Physics Letters* 2014, **104**, 143901.
- 65 N. H. Alvi, PED Soto Rodriguez, Praveen Kumar, V. J. Gomez, P. Aseev, A. H. Alvi, M. A. Alvi, Magnus Willander, and R. Nötzel, *Applied Physics Letters*, 2014, **104**, 223104; B. AlOtaibi, M. Harati, S. Fan, S. Zhao, H. P. T. Nguyen, M. G. Kibria, and Z. Mi. *Nanotechnology* 2013, **24**, 175401.
- 66 M. G. Kibria, F. A. Chowdhury, S. Zhao, B. AlOtaibi, M. L. Trudeau, H. Guo, and Z. Mi. *Nature communications* 2015, **6**, 6797
- 67 J.-H. Ryou, P.D. Yoder, J. Liu, Z. Lochner, H. Kim, S. Choi, H.J. Kim, and R.D. Dupuis, *Selected Topics in Quantum Electronics, IEEE Journal*, 2009, **15**(4), 1080-1091.
- 68 Z.Q. Li, M. Lestrade, Y.G. Xiao, and S. Li., *physica status solidi (a)*, 2011, **208**(4), 928-931.
- 69 C. Fabien, A.M Chloe, and W.A. Doolittle, *Solar Energy Materials and Solar Cells*, 2014, **130**, 354-363.
- 70 H. Masui, S. Nakamura, S.P. DenBaars, and U.K. Mishra, *Electron Devices, IEEE Transactions*, 2010, **57**(1), 88-100.

- 71 K. Maeda, T. Takata, M. Hara, N. Saito, Y. Inoue, H. Kobayashi, and K. Domen, *Journal of the American Chemical Society*, 2005, **127**(23), 8286-8287.
- 72 M.A. Moram and S. Zhang, *Journal of Materials Chemistry A*, 2014, **2**(17), 6042-6050.
- 73 M. Akiyama, K. Kano, and A. Teshigahara, *Applied Physics Letters*, 2009, **95**(16), 162107
- 74 H. Peng, P.F. Ndione, D.S. Ginley, A. Zakutayev, and S. Lany, *Phys. Rev. X*, 2015, **5**, 021016.
- 75 P. Narang, S. Chen, N.C. Coronel, S. Gul, J. Yano, L.-W. Wang, N.S. Lewis, and H.A. Atwater, *Advanced Materials*, 2014, **26**(8), 1235-1241; P.C. Quayle, K. He, J. Shan, and K. Kash, *MRS Communications*, 2013, **3**(3), 135-138.
- 76 L. Lahourcade, N.C. Coronel, K.T. Delaney, S.K. Shukla, N.A. Spaldin, and H.A. Atwater, *Advanced Materials*, 2013, **25**(18), 2562-2566; S. Chen, P. Narang, H.A. Atwater, and L.-W. Wang, *Advanced Materials*, 2014, **26**(2), 311-315.
- 77 A.N. Fioretti, A. Zakutayev, H. Moutinho, C. Melamed, J.D. Perkins, A.G. Norman, M. Al-Jassim, E.S. Toberer, and A.C. Tamboli, *Journal of Materials Chemistry C*, 2015, **3**(42), 11017-11028.
- 78 N. Feldberg, J.D. Aldous, W.M. Linhart, L.J. Phillips, K. Durose, P.A. Stampe, R.J. Kennedy, et al., *Applied Physics Letters*, 2013, **103**(4), 042109.
- 79 T. D. Veal, N. Feldberg, N. F. Quackenbush, W.M. Linhart, D.O. Scanlon, L.F. Piper, and S.M. Durbin, *Advanced Energy Materials*, 2015, 10.1002/aenm.201501462
- 80 H. Katagiri, K. Jimbo, W.S. Maw, K. Oishi, M. Yamazaki, H. Araki, and A. Takeuchi, *Thin Solid Films*, 2009, **517**(7), 2455-2460.
- 81 H. Kawazoe, M. Yasukawa, H. Hyodo, M. Kurita, H. Yanagi, and H. Hosono, *Nature*, 1997, **389**(6654), 939-942.
- 82 U. Zachwieja and H. Jacobs, *Eur. J. Solid State Inorg. Chem.*, 1991, **28**, 1055-1062.
- 83 M. Yang, A. Zakutayev, J. Vidal, X. Zhang, D.S. Ginley, and F.J. DiSalvo, *Ener. Envir. Sci.*, 2013, **6**, 2994.
- 84 A. Zakutayev, A.J. Allen, X. Zhang, J. Vidal, Z. Cui, S. Lany, M. Yang, F.J. DiSalvo, and D.S. Ginley, *Chem. Mater.*, 2014, **6**, 4970.
- 85 I. Ohkubo and T. Mori, *Chemistry of Materials* (2015).
- 86 R. Niewa and F.J. DiSalvo, *J. Alloys Compd.*, 1998, **279**, 153-160; F.J. DiSalvo, S.S. Trail, H. Yamane, and N.E. Brese, *J. Alloys Compd.*, 1997, **255**, 122-129.
- 87 A. Zakutayev, V. Stevanovic, and S. Lany, *Applied Physics Letters*, 2015, **106**(12), 123903; L.L. Baranowski, P.P. Zawadzki, S.T. Christensen, D. Nordlund, S. Lany, A.C. Tamboli, L. Gedvilas, D.S. Ginley, W. Tumas, E.S. Toberer, and A. Zakutayev, *Chemistry of Materials*, 2014, **26**(17), 4951-4959; A. Zakutayev, D.H. McIntyre, G. Schneider, R. Kykyneshi, D.A. Keszler, C.-H. Park, and J. Tate, *Thin Solid Films*, 2010, **518**(19), 5494-5500.
- 88 X. Zhang, L. Yu, A. Zakutayev, and A. Zunger, *Advanced Functional Materials*, **22**(7), 1425-1435.
- 89 Y. Wu, P. Lazic, G. Hautier, K. Persson, and G. Ceder, *Energy & Environmental Science*, 2013, **6**(1), 157-168; G. Hautier, C. Fischer, V. Ehrlacher, A. Jain, and G. Ceder, *Inorg. Chem.*, 2011, **50**, 656-663.
- 90 R.E. Schaak and T.E. Mallouk, *Chemistry of Materials*, 2002, **14**(4), 1455-1471; J. Mannhart and D.G. Schlom, *Science*, 2010, **327**(5973), 1607-1611.
- 91 A.S. Bhalla, R. Guo, and R. Roy, *Material Research Innovations*, 2000, **4**(1), 3-26.
- 92 S. Y. Yang, J. Seidel, S. J. Byrnes, P. Shafer, C.H. Yang, M. D. Rossell, P. Yu, Y.-H. Chu, J. F. Scott, J. W. Ager, III, L. W. Martin, and R. Ramesh, *Nature nanotechnology*, 2010, **5**(2), 143-147.
- 93 R. Nechache, C. Harnagea, S. Li, L. Cardenas, W. Huang, J. Chakrabarty, and F. Rosei, *Nature Photonics*, 2015, **9**(1), 61-67.
- 94 M.M. Lee, J. Teuscher, T. Miyasaka, T.N. Murakami, and H.J. Snaith, *Science*, 2012, **338**(6107), 643-647.
- 95 N.E. Brese and F.J. DiSalvo, *Journal of Solid State Chemistry*, 1995, **120**(2), 378-380; V.V. Bannikov, I.R. Shein, and A.L. Ivanovskii, *physica status solidi (RRL)-Rapid Research Letters*, 2007, **1**(3), 89-91.
- 96 R. Sarmiento-Pérez, T.F.T. Cerqueira, S. Körbel, S. Botti, and M.A.L. Marques, *Chemistry of Materials*, 2015, **27**(17), 5957-5963.
- 97 P. Bacher, P. Antoine, R. Marchand, P. L'Haridon, Y. Laurent, and G. Roullet, *Journal of Solid State Chemistry*, 1988, **77**(1), 67-71.
- 98 S.G. Ebbinghaus, H.-P. Abicht, R. Dronskowski, T. Müller, A. Reller, and A. Weidenkaff, *Progress in Solid State Chemistry*, 2009, **37**(2), 173-205.
- 99 I.E. Castelli, T. Olsen, S. Datta, D.D. Landis, S. Dahl, K.S. Thygesen, and K.W. Jacobsen, *Energy & Environmental Science*, 2012, **5**(2), 5814-5819.
- 100 M. Yang, J. Oró-Solé, J.A. Rodgers, A. Belén Jorge, A. Fuertes, and J.P. Attfield, *Nature Chemistry*, 2011, **3**(1), 47-52

Nitride semiconductors have properties suitable for solar energy conversion and can be synthesized using high-energy precursors

